Delayed rectifier current of bullfrog sympathetic neurons: ion–ion competition, asymmetrical block and effects of ions on gating

Brian M. Block and Stephen W. Jones*†

*Department of Neurosciences and *Department of Physiology & Biophysics, Case Western Reserve University, Cleveland, OH 44106, USA*

1. The delayed rectifier (DR) K^+ channel pore was probed using different permeant and blocking ions applied intra- and extracellularly. Currents were recorded from bullfrog sympathetic neurons using whole-cell patch-clamp techniques.

2. With intra- and extracellular Cs^+ (0 K^+), there were large, tetraethylammonium (TEA)-sensitive currents. Adding K^+ back to the extracellular solution revealed that the current with Cs_i^+ was K^+ selective (permeability ratio $P_{Cs}/P_K = 0{\cdot}17 \pm 0{\cdot}02$, $n = 4$) and showed a strong anomalous mole fraction effect.

3. There were also large non-inactivating currents with Na_i^+ and Na_o^+ (0 K^+). The current with Na_i^+ was K^+ selective (Na_o^+ *vs.* K_o^+: $P_{Na}/P_K = 0{\cdot}022 \pm 0{\cdot}005$, $n = 5$), and was TEA sensitive with K_o^+ but not with Na_o^+.

4. Permeant ions affected gating kinetics. DR currents activated faster in K^+ than in Cs^+, and activated faster with increasing concentrations of either K^+ or Cs^+. Deactivation was slowed by increased K^+ or Cs^+ concentration, with no difference between K^+ and Cs^+.

5. The pore was also characterized using intracellular blocking ions. A wide variety of monovalent cations (TEA, *N*-methyl-D-glucamine, arginine, choline, $CH_3NH_3^+$, Li^+, Cs^+ and Na^+) blocked DR channels from the inside in a voltage-dependent manner: K_D at 0 mV was 2·9 mM for TEA and 134–487 mM for the others, at apparent electrical distances (δ) of 0·33–0·79. There was no detectable block by 10 mM Mg_i^{2+}. Apart from TEA, the organic cations did not block from the outside.

6. The permeability to Na^+ in the absence of K^+, and the strong anomalous mole fraction effects observed for $Cs_o^+ + K_o^+$ mixtures, suggest that DR channels select for K^+ using ion–ion competition. The block by large intracellular cations shows that the pore is asymmetrical. The loss of high affinity TEA_o block with Na_i^+ and Na_o^+, and the effects of permeant ions on gating, suggest that channel conformation may be affected by ions in the pore.

Much work has been done using both conducting and blocking ions to characterize the ion-conducting pore of K^+ channels (Hille, 1992). K^+ channels are highly selective for K^+ over Na^+, often 100-fold or greater, and yet can conduct over 10^6 ions per second, both crucial properties for their physiological role. K^+ channels are thought to be single-file pores that can contain multiple ions simultaneously, which allows both high selectivity and large ion fluxes (Hille, 1992; Stampe & Begenisich, 1996). Both permeant and blocking cations can provide information about mechanisms of permeation. Small inorganic ions such as Cs^+ can probe the narrowest part of a K^+ channel, while large organic cations probe the wider regions along the conduction pathway.

We previously studied currents through the delayed rectifier (DR) K^+ channel of bullfrog sympathetic neurons, using physiological K_i^+ (88 mM), and varying the extracellular ions. The DR channel could carry a small Na^+ current, was a multi-ion pore, and was blocked by both Na_o^+ and Cs_o^+ (Block & Jones, 1996*a*). Here we continue our study of DR channel permeation by varying the internal ions. One motive for this work was the recent observation that Na^+ carries large currents through some K^+ channels when K_i^+ is removed (Zhu & Ikeda, 1993; Callahan & Korn, 1994; Korn & Ikeda, 1995). Therefore, we measured DR channel permeation properties in the absence of K_i^+. Both Cs^+ and Na^+ carry large currents in the absence of K^+, and with Cs_i^+ there is a

† To whom correspondence should be addressed.

dramatic anomalous mole fraction effect in mixtures of Cs_o^+ and K_o^+. We also found that impermeant intracellular cations, both organic and inorganic, can block the channel in a voltage-dependent manner. Preliminary results of this project have been reported (Block & Jones, 1996*b*).

METHODS

Cells and recording conditions

Neurons were isolated as previously described (Kuffler & Sejnowski, 1983; Jones, 1987; Block & Jones, 1996*a*). Briefly, adult bullfrogs (*Rana catesbeiana*) were decapitated and pithed, caudal paravertebral sympathetic ganglia were excised, and neurons were enzymatically dissociated. Isolated cells were stored in supplemented L15 culture medium at 4 °C for up to 2 weeks. Large spherical neurons (49 ± 1 pF, range 24–104 pF, $n = 155$) were used for recordings. Patch-clamp recordings were made at room temperature (22–24 °C) in the whole-cell configuration using electrodes pulled from EN-1 glass (Garner Glass, Claremont, CA, USA).

Currents were recorded with an Axopatch-200 amplifier (Axon Instruments), Labmaster A–D interface (Axon Instruments), and 8-pole Bessel low-pass filter (Frequency Devices, Haverhill, MA, USA), and stored on a personal computer. The sampling frequency was 5 or 10 kHz with 2 or 3 kHz analog filtering, respectively. pCLAMP software (Axon Instruments) was used for data acquisition.

Whole-cell series resistance (R_S) was estimated from optimal correction of the capacity transient. The R_S varied with the conductivity of the intracellular solution, with average R_S (before compensation) of 1·8 ± 0·1 MΩ ($n = 21$) with 25 mM $K_i^+ + NMG_i$, 5·2 ± 0·3 MΩ ($n = 18$) with 25 mM $K_i^+ + \text{sucrose}_i$, and 1·6 ± 0·1 MΩ ($n = 30$) with 120 mM K_i^+. R_S compensation was set to 80% (prediction) and 95% (correction). We estimate that the actual steady-state compensation was approximately 80%, based on simulations of the effect of R_S error on tail current waveforms using a kinetic model for DR current (K. G. Klemic & S. W. Jones, unpublished observations), and on measurements from model cells. For 25 mM $K_i^+ + NMG_i$ in a 50 pF cell, 0·4 MΩ of uncompensated series resistance would produce a 0·4 mV nA^{-1} steady-state voltage error and a 20 μs time constant for the voltage clamp. The voltage error and clamp time constant would be approximately 3-fold larger when using 25 mM K_i^+ + intracellular sucrose. All R_S values listed in the text are for R_S before compensation, and estimates of the voltage error (mV nA^{-1}) assume 80% compensation.

Solutions

Solution compositions are listed in Table 1. Chemicals were purchased from Sigma except for saxitoxin (Calbiochem, La Jolla, CA, USA), and CsCl (Fisher Scientific, Pittsburgh, PA, USA). Except for glucosamine (discussed below), the pK_a values for the organic cations were ⩾ 8·9, so they were > 98% ionized at pH 7·2 (Juvet, 1959; Jukes, 1964; Martell & Smith, 1975).

Extracellular solutions were changed by a 'sewer pipe' fast flow system, unless noted otherwise. The pipes were deactivated fused silica tubing (0·32 mm inner diameter; J & W Scientific, Folsom, CA, USA) held together with Sylgard (Dow Corning). Cells were placed within 100 μm of the pipe opening. Previous studies have shown rapid (< 1 s) and complete solution exchange with this type of flow system (Jones, 1991).

Junction potentials

Before forming a seal with the membrane, the patch pipette current was manually adjusted to zero with a 3 M KCl–agar bridge as reference. In these conditions, there are two sources of junction potentials: the electrode–bath junction, and the junction between the outflow of a flow pipe and the bath. When possible, solutions were selected to minimize those junction potentials. For experiments using 100 mM Cs_i^+, 100 mM Na_i^+ or 120 mM K_i^+, the electrode was zeroed with 2·5 mM $K_o^+ + Na_o^+$ in the bath to match the pipette solution and the 120 mM Na_o^+, Cs_o^+, or K_o^+ in the fast flow system. Experiments on internal cation block used 2·5 mM $K_o^+ + NMG_o$ in the bath and 25 mM $K_o^+ + NMG_o$ in the fast flow system. Junction potentials were measured with standard methods (Barry & Lynch, 1991; Neher, 1992) using the patch-clamp amplifier in current-clamp mode. The voltage was set to zero with the same solution present in both the electrode and the bath, the junction potential was measured after changing the bath to the solution to be tested, and the bath was then changed back to the initial solution to check for drift. There was a large junction potential for 25 mM K_i^+ + intracellular sucrose relative to 2·5 mM $K_o^+ + NMG_o$ (+24·8 mV; convention of Barry & Lynch, 1991); other junction potentials were less than ±10·4 mV. The voltages shown in the figures are the voltage commands after correcting for junction potentials.

Current isolation

Solutions were designed to isolate DR current by replacing Na^+ in the extracellular solution with *N*-methyl-D-glucamine (NMG), and by replacing extracellular Ca^{2+} with Mn^{2+} to prevent Ca^{2+} currents and Ca^{2+}-activated K^+ currents. Where Na^+- or Li^+-containing solutions were used, the depolarizing step given to activate DR current (90 ms at +60 mV) inactivated Na^+ currents before measurements or hyperpolarizing steps were made. Where noted, 1 μM saxitoxin was added to the extracellular solution to block Na^+ channels (Jones, 1987). Bullfrog sympathetic neurons have M-type and occasionally A-type K^+ currents. M-current amplitude is at most one-tenth of the amplitude of DR current (Block & Jones, 1996*a*), and tends to run down strongly without internal phosphocreatine, so it would have little effect on the measurements here. A-current is mostly inactivated at a holding potential of −80 mV (Adams, Brown & Constanti, 1982), and rapidly inactivating A-like currents were not observed in these experiments. Additionally, current amplitudes for determination of E_{rev}, conductance and ion block were measured after any A-current would have inactivated, either late in the depolarizing step or from the subsequent tail currents. The adequacy of current isolation, and the use of difference currents ± TEA, are discussed further below.

Analysis

Currents were analysed using pCLAMP (versions 5.5 and 6.0; Axon Instruments) and Excel software (version 5.0; Microsoft, Redmond, WA, USA). Currents were leak-subtracted using inverted steps of one-quarter amplitude, with four records averaged and scaled. Alternatively, where noted, the TEA-sensitive current was used, defined as the total current minus the current remaining in 10 mM TEA_o. Instantaneous *I–V* relationships were measured from tail current amplitudes (Fig. 1*A*, arrow), averaged between 0·5–0·6 and 1 ms after repolarization from a 90 ms step to +60 mV. The step to +60 mV maximally activated DR current (Block & Jones, 1996*a*).

For all measurements involving changes in extracellular solutions, test conditions were compared with measurements made both before and after the test. Control was then defined as the mean of measurements before and after.

Table 1. Composition of intracellular (pipette) and extracellular solutions (mM)

	Intracellular solutions						Extracellular solutions				
	100 X^+	100 X^+ + 25 K^+	25 K^+ + NMG	25 K^+ + sucrose	120 K^+	Glucosamine	120 X^+	80 X^+	25 K^+ + NMG	25 K^+ + sucrose	2·5 K^+ + NMG
XCl	100	100	—	—	—	—	120	80	—	—	—
KCl	—	—	25	—	95	—			25	25	2·5
NMG-Cl	—	—	75	—	—	—	—	40	92·5	—	115
NMG–EGTA	10	—	10	—	—	—	—	—	—	—	—
K_2-EGTA	—	10	—	10	10	6	—	—	—	—	—
$MgCl_2$	4	4	4	4	4	4	—	—	—	—	—
NMG–Hepes	2·5	2·5	2·5	2·5	2·5	2·5	2·5	2·5	2·5	2·5	2·5
Tris–ATP	5	5	5	5	5	5	—	—	—	—	—
KOH	—	5	—	5	5	5	—	—	—	—	—
NMG base	5	—	5	—	—	—	—	—	—	—	—
K_x-glucosamine	—	—	—	—	—	50	—	—	—	—	—
Sucrose	—	—	—	200	—	142	—	—	—	185	—
$MnCl_2$	—	—	—	—	—	—	2	2	2	2	2

For TEA_o subtraction, 10 mM TEA was added to the extracellular solution. For TEA_i solutions, 1 mM TEA was added to 25 mM K_i^+ + intracellular sucrose. Glucosamine stock solution (1 M) was made freshly each day by titrating glucosamine–HCl with ~0·2 mol KOH (mol glucosamine)$^{-1}$. To maintain $[K^+]_i$ at 25 mM for the intracellular glucosamine solution, K_2-EGTA was reduced to 6 mM and only 50 mM intracellular glucosamine was used, with sucrose added for osmolality. For the extracellular glucosamine solution, 92·5 mM glucosamine replaced NMG in 25 mM K_o^+ + NMG_o and KCl was reduced to keep $[K^+]_o$ at 25 mM. NMG-Cl was prepared by the addition of ~1 mol HCl (mol NMG base)$^{-1}$, and the NMG–Hepes stock was prepared by the titration of Hepes to pH 7·2 with ~0·5 mol NMG base (mol Hepes)$^{-1}$. Tris–ATP contained 2·5 mol Tris (mol ATP)$^{-1}$. If necessary, the pH of the internal solutions was adjusted to 7·2 with a small amount of NMG base.

Ion selectivity was assessed under conditions where the extracellular solution contained only a single permeant ion at a time. DR channel permeability ratios were determined in extracellular solutions where the only cations were Mn^{2+}, NMG, and the ion of interest (either X^+ + NMG, or 120 mM X^+). Permeability ratios (P_X/P_K) were calculated from the shift in reversal potentials (E_{rev}) between ions, using a version of the Goldman–Hodgkin–Katz voltage equation (eqns 13–17 of Hille, 1992):

$$\Delta E_{rev} = (RT/F)\ln((P_X[X^+]_o)/(P_K[K^+]_o)). \quad (1)$$

Chord conductances (G) were defined by:

$$G = I/(V - E_{rev}), \quad (2)$$

and were calculated from the 'instantaneous' tail currents.

Voltage-dependent block was quantified with a simplified version of the Woodhull (1973) model, assuming that the blocking ion binds to a single site in the membrane field, and cannot permeate the channel. Under conditions where the instantaneous I–V relationship is linear:

$$I = G(V - E_{rev})(1 + [X^+]_i(K_{D0}\exp(-z\delta FV/RT))^{-1})^{-1}. \quad (3)$$

There are four free parameters to the model: conductance (G), E_{rev}, dissociation constant at 0 mV (K_{D0}), and apparent electrical distance (δ). F, R, z and T have their usual meanings. Experimentally observed instantaneous I–V relationships were fitted to eqn (3) using the Solver function of Excel, which uses a generalized reduced gradient method to optimize the parameters. The best fit was determined by minimizing the sum of the squared errors.

Current kinetics were evaluated by fitting exponentials to the time course of activation during depolarization, or deactivation (tail currents) upon repolarization, using Clampfit software (version 6.0; Axon Instruments). Activation was approximated by a single exponential fitted to the data over the time period from 50% of the maximal current amplitude to the end of the 90 ms step. This procedure avoids the initial sigmoidal delay in channel activation, and is used because the entire time course of activation is not well described by a power law, or by the sum of two exponentials (Greene & Jones, 1993; K. G. Klemic & S. W. Jones, unpublished observations). Tail currents were fitted to either one or two exponentials. When the currents were reasonably well described by a single exponential, two exponential fits often gave inconsistent results, especially using the Chebychev method within the Clampfit program. In such cases, the Simplex or 'mixed' methods were used. For estimation of the relative amplitudes of fast and slow components of tail currents, the time constants were fixed to values estimated for the main tail components present in the TEA-sensitive and TEA-resistant currents.

Differences between experimental conditions were evaluated with two-tailed Student's t tests, with $P < 0·05$ considered to be significant, and using Bonferroni's correction for multiple tests. When comparing measurements in the same set of cells, a paired t test was used. Values presented are means ± S.E.M.

Table 2. Block by 10 mM TEA_o in different ionic conditions

Internal ion	External ion	Fraction blocked at +60 mV	Fraction blocked at −80 mV	n
100 mM Cs^+	120 mM Cs^+	0·68 ± 0·01	0·73 ± 0·01	10
	1 mM K^+ + 119 mM Cs^+	0·65 ± 0·04	0·70 ± 0·01	8
	25 mM K^+ + 95 mM K^+	0·74 ± 0·02	0·73 ± 0·01	8
	120 mM K^+	0·75 ± 0·05	0·76 ± 0·02	7
120 mM K^+	120 mM Cs^+	0·75 ± 0·01	0·76 ± 0·03	5
	1 mM K^+ + 119 mM Cs^+	0·77 ± 0·03	0·78 ± 0·03	4
	25 mM K^+ + 95 mM K^+	0·78 ± 0·03	0·83 ± 0·02	4
	120 mM K^+	0·78 ± 0·01	0·78 ± 0·01	12
100 mM Na^+	2·5 mM K^+	0·58 ± 0·02	0·70 ± 0·02	3

RESULTS

Currents with Cs^+

Given recent reports that some K^+ channels can carry large Cs^+ and Na^+ currents in the absence of K_i^+ (Zhu & Ikeda, 1993; Callahan & Korn, 1994; Korn & Ikeda, 1995), and the observation that DR channels carried small Na^+ and Cs^+ currents even with K_i^+ (Block & Jones, 1996*a*), it has been hypothesized that DR Cs^+ and Na^+ currents would be larger in the absence of K_i^+. Replacement of K^+ with Cs^+ resulted in substantial inward and outward currents (Fig. 1). The main issue was to verify that the current carried by Cs^+ was through DR channels. Like DR currents with K_i^+ and K_o^+, most of the current with Cs_i^+ and Cs_o^+ was sensitive to tetraethylammonium (TEA). The dose–response relationship was well described by a K_D value of 3·4 mM and maximal inhibition of 0·88 (Fig. 1*C*), compared with a K_D value of 1·8 mM and maximal inhibition of 0·95 for current with K^+

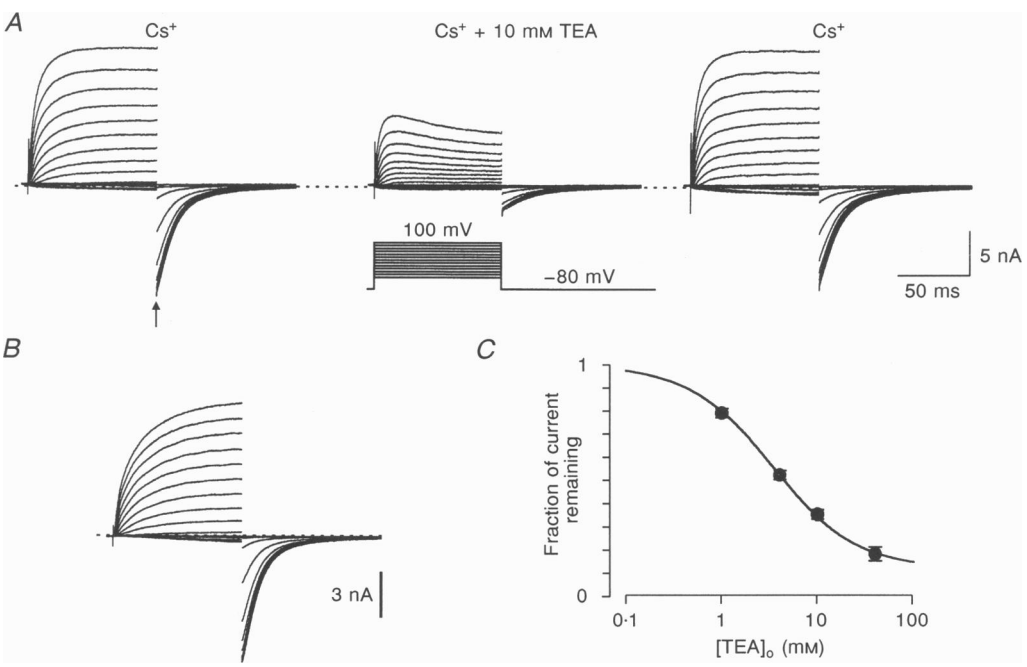

Figure 1. Currents with 100 mM Cs_i^+ and 120 mM Cs_o^+

A, leak-subtracted traces, recorded before, during and after addition of 10 mM TEA_o (left to right, respectively). Here, and in all other figures, the dashed line indicates zero current, and the first 0·5 ms of the tail currents is blanked. The arrow points to where the 'instantaneous' tail currents were measured. *B*, TEA-sensitive current, calculated as the average of currents before and after TEA, minus the current in 10 mM TEA_o. Data in *A* and *B* are from cell b5o20 (R_S = 2·1 MΩ). *C*, blockade of tail currents by TEA_o. Solutions contained 100 mM Cs_i^+ and 80 mM Cs_o^+, plus 40 mM total TEA_o + NMG_o. Tail currents were measured at −80 mV after a 90 ms step to +40 mV. A single-site binding curve was fitted to the data (K_D = 3·4 mM, maximal inhibition = 0·88).

(Greene & Jones, 1993). Also like DR currents with K^+, external TEA block was not measurably voltage dependent (Table 2). The current resistant to TEA has not been characterized in detail, but it appears to be kinetically distinct from the main DR current. The TEA-resistant current activated more rapidly than the TEA-sensitive current, and the resistant current often inactivated slightly during 90 ms steps to strongly depolarized voltages (Fig. 1*A*). This inactivation does not reflect a time-dependent blocking action of TEA, as difference currents using different concentrations of TEA activated with the same time course (Fig. 2*B*), which would not be expected if TEA introduced concentration-dependent kinetics. The total tail current with Cs^+ had fast and slow components ($\tau = 9{\cdot}4 \pm 0{\cdot}4$ ms and $29{\cdot}4 \pm 4{\cdot}6$ ms at −80 mV in one set of four cells), and the fast component was selectively blocked by TEA (Fig. 2). The dose–response relationships for the fast and slow tail components analysed separately gave a K_D value of 3·6 mM for the fast tails, and 56 mM for the slow tails, with 84% of the total tail current being the faster component. Thus the kinetic and pharmacological methods of current separation (fast *vs.* slow tails; TEA-sensitive *vs.* TEA-resistant tails) gave nearly identical results. The K_D for TEA block of the slow component may not be estimated accurately, as the highest TEA concentration used produced less than 50% block, but the slow component was clearly much less sensitive to TEA. Like DR currents in K^+, the TEA-sensitive current in Cs^+ was non-inactivating (over 90 ms) and activated with a delay (Figs 1*B* and 2*B*). The current with Cs^+ activated more slowly than with K^+, but deactivation kinetics and steady-state activation were similar to that with K^+ (Table 3; see Fig. 5). Based on this evidence, it is concluded that ~85% of the whole-cell current with Cs^+ is a TEA-sensitive current carried by the DR channel. The difference current ±10 mM TEA should be > 90% of the DR current, as this concentration produces strong block of the fast tail component with little or no effect on the slow component (Fig. 2*C*).

DR channels were K^+ selective with 100 mM Cs^+_i. Permeability was determined from reversal potentials (eqn (1)), comparing 120 mM Cs^+_o with K^+_o. The permeability ratio was the same whether measured from the total current or the TEA-sensitive current ($P_{Cs}/P_K = 0{\cdot}17 \pm 0{\cdot}02$, $n = 4$).

Many K^+ channels have an anomalous mole fraction effect in mixtures of permeant ions (Hille, 1992). Figure 3 shows that the TEA-sensitive inward current with Cs^+ was reversibly blocked by adding 1 or 25 mM K^+ to the extracellular solution, and the current was much larger in 120 mM K^+_o than in Cs^+_o. The chord conductance (G_{chord}) showed a strong anomalous mole fraction effect whether measured at fixed driving force (Fig. 3*C*, ◆) or at a fixed voltage (Fig. 3*C*, ◇). The instantaneous current with 25 mM K^+_o + 95 mM Cs^+_o had a region of near-zero slope (Fig. 3*B*), so G_{chord} depended on the voltage where it was measured. The DR current showed a qualitatively similar but less dramatic anomalous mole fraction effect with 120 mM K^+_i, in mixtures of K^+_o and Cs^+_o (data not shown). The robust anomalous mole fraction effects confirm our previous conclusion that the DR channel is a multi-ion pore (Block & Jones, 1996*a*).

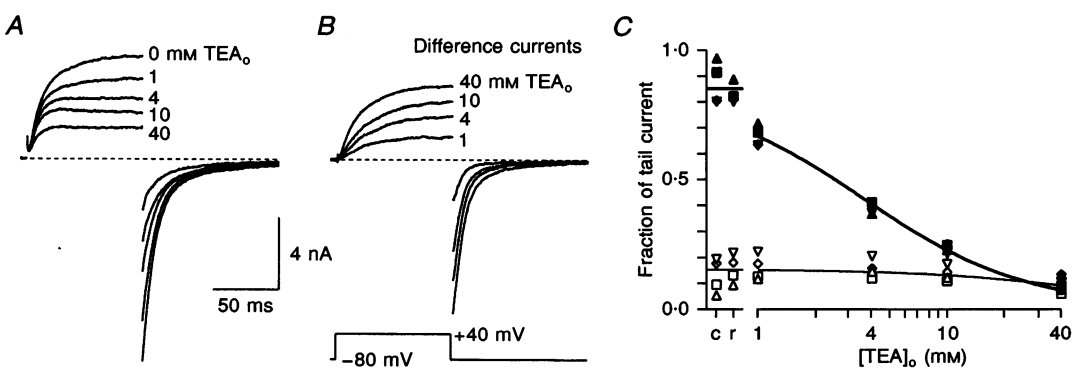

Figure 2. Sensitivity of Cs^+ tail current components to TEA_o

Data are for solutions containing 100 mM Cs^+_i and 80 mM Cs^+_o, as in Fig. 1*C*. *A*, leak-subtracted currents recorded at the indicated $[TEA]_o$. TEA concentrations were applied in increasing order, with 94% recovery after wash in this cell (not shown). Cell c5o09, $R_S = 1{\cdot}5$ MΩ. *B*, difference currents, calculated as in Fig. 1*B*, from the data of *A*. In four cells, time constants for activation (approximated by a single exponential, see Methods) were $26{\cdot}7 \pm 3{\cdot}6$ ms (1 mM TEA), $29{\cdot}0 \pm 2{\cdot}2$ ms (4 mM), $27{\cdot}0 \pm 1{\cdot}7$ ms (10 mM) and $20{\cdot}6 \pm 0{\cdot}8$ ms (40 mM). As the TEA-resistant current is partially inhibited at 40 mM, the slightly faster time constant at 40 mM may reflect a contribution of TEA-resistant current. *C*, dose–response relationships for fast and slow components of tail currents at −80 mV, following steps to +40 mV. Fast and slow amplitudes are denoted by the filled and open symbols, respectively. The relative amplitudes recorded in control conditions (c) and after recovery (r) are shown on the left. Tail currents were fitted to the sum of two exponentials, with time constants fixed to values chosen to describe the tail currents at all TEA concentrations. The fast time constants were close to those from unconstrained single exponential fits to difference currents ± TEA, and the slow time constants to the currents remaining in 40 mM TEA.

Table 3. Steady-state activation parameters in different ionic conditions

Internal	External	z	$V_{½}$ (mV)	n
100 mM Cs^+	120 mM Cs^+	2·7 ± 0·2	−3·7 ± 1·3	4
100 mM Na^+	120 mM Na^+	1·7 ± 0·5	−4·9 ± 1·2	8
100 mM Na^+	2·5 mM K^+ + NMG	3·4 ± 0·2	1·9 ± 1·3	4
88 mM K^+	15 mM K^+	1·7 ± 0·1	2·0 ± 2·1	6

Tail currents were measured after depolarizations lasting 90 ms. Tail amplitudes were fitted to a Boltzmann relation:

$$I = I_{max}/(1 + \exp((V_{½} - V)zF/(RT))). \quad (4)$$

Difference currents ± TEA were used for data with Cs^+, and for Na_i^+ with K_o^+ + NMG_o. Leak-subtracted currents were used for the other conditions. The data with K_i^+ and K_o^+ are from Block & Jones (1996*a*).

Cs^+ and K^+ currents were also compared using the same permeant ion on both sides of the membrane. At +60 mV, current amplitude with 100 mM Cs_i^+ and 120 mM Cs_o^+ was 0·13 ± 0·01 nA pF^{-1} ($n = 9$), which was significantly smaller than the current with 120 mM K_i^+ and 120 mM K_o^+ (1·03 ± 0·24 nA pF^{-1}, $n = 3$). The value with 120 mM K_i^+ and K_o^+ was underestimated by ~30% because of R_S error.

Currents with Na^+

As with Cs^+, non-inactivating currents were observed with 100 mM Na_i^+ and 120 mM Na_o^+, in the absence of K^+ (Fig. 4*A*; also note the rapidly inactivating currents through Na^+ channels). The current with Na^+ (0·07 ± 0·01 nA pF^{-1} at +60 mV, $n = 7$) was significantly smaller than with either K^+ or Cs^+. Steady-state activation was similar to that of DR current carrying K^+ (Table 3). The current with Na_i^+ was K^+ selective (Fig. 4). Comparing 120 mM Na_o^+ with 2·5 mM K_o^+ + 117·5 mM NMG_o, P_{Na}/P_K was 0·022 ± 0·005 ($n = 5$). Interestingly, 10 mM TEA_o only blocked 14 ± 3% of the non-inactivating current with Na_o^+ ($n = 9$), but the current with 2·5 mM K_o^+ + 117·5 mM NMG_o was TEA sensitive (Fig. 4; Table 2). The simplest interpretation is that most of the non-inactivating current with Na^+ as the charge carrier was the DR current (for similar findings, see Ikeda & Korn, 1995; Korn & Ikeda, 1995).

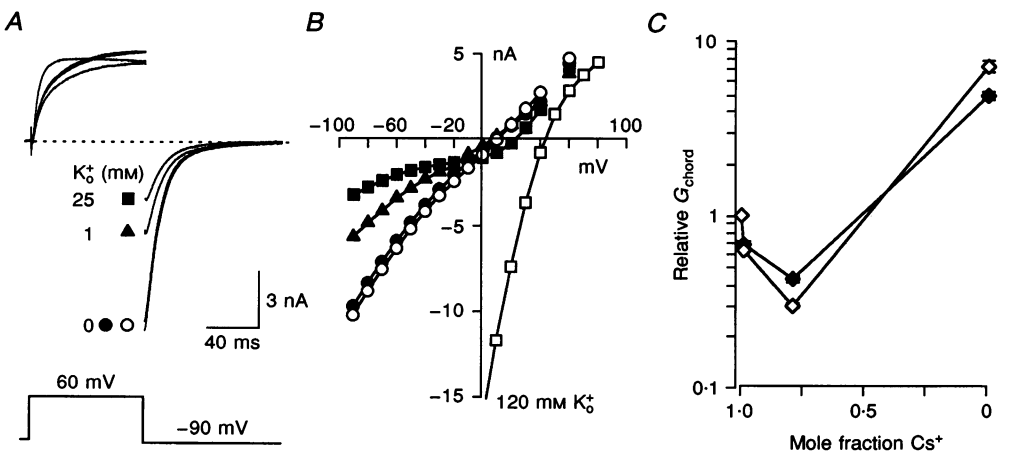

Figure 3. Anomalous mole fraction effects with 100 mM Cs_i^+ and mixtures of K_o^+ and Cs_o^+

The sum of $[K^+]_o$ and $[Cs^+]_o$ was 120 mM, with only the $[K^+]_o$ indicated in the figure. *A*, with 100 mM Cs_i^+, TEA-sensitive inward currents were reduced in 1 mM K_o^+ + 119 mM Cs_o^+, and 25 mM K_o^+ + 95 mM Cs_o^+, compared with 120 mM Cs_o^+ (control and recovery). *B*, instantaneous *I–V* relationships from the same cell as in *A*. Note the near-zero slope region for the 25 mM K_o^+ + 95 mM Cs_o^+ data. Cell b5o20. *C*, relative chord conductance (G_{chord}) in the mixtures of K_o^+ and Cs_o^+, with 100 mM Cs_i^+. G_{chord} was calculated 30 mV negative to E_{rev} (◆) or at −60 mV (◇), and was normalized to the value in 120 mM Cs_o^+. Error bars are shown when larger than the symbols. For the cell in *B*, R_S was 2·1 MΩ, giving a voltage error of ~0·4 mV nA^{-1} assuming 80% compensation. Currents in Cs^+ could be clamped well even at −100 mV, but R_S error was significant at negative voltages in 120 mM K_o^+, so the measured G_K/G_{Cs} of 7·3 ± 0·6 at −60 mV ($n = 3$) would underestimate the true G_K/G_{Cs}.

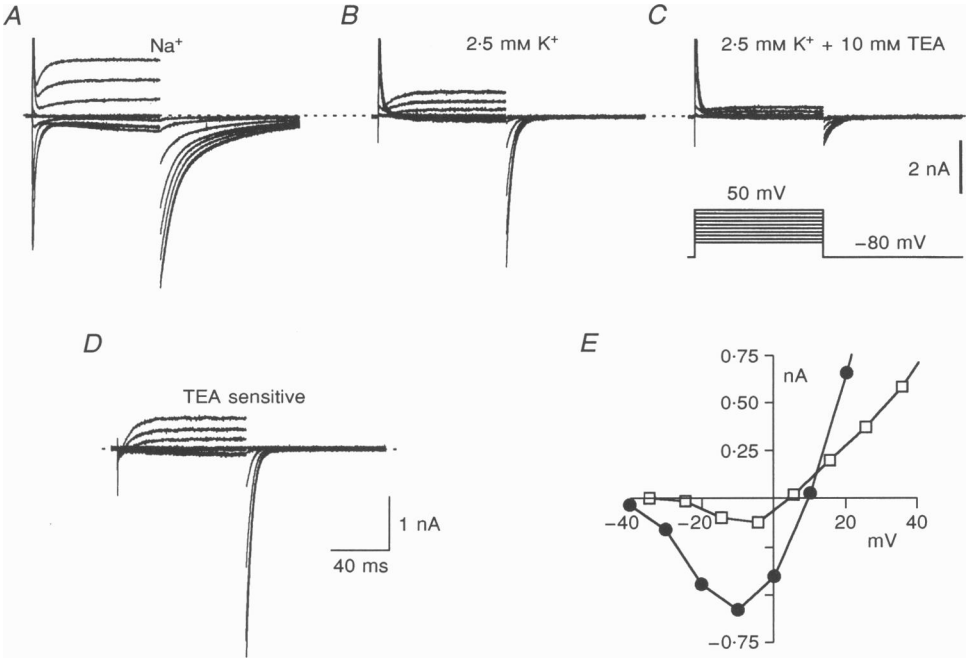

Figure 4. Currents with 100 mM Na_i^+

A, currents with 120 mM Na_o^+. *B*, currents with 2·5 mM K_o^+ + NMG_o. *C*, block of both inward K^+ current and outward Na^+ current by 10 mM TEA_o, with 2·5 mM K_o^+ + NMG_o. Records in *A*, *B* and *C* are leak-subtracted. *D*, the TEA-sensitive current (*B* minus *C*) with 100 mM Na_i^+ and 2·5 mM K_o^+ + NMG_o. *E*, steady-state *I–V* relationships in 120 mM Na_o^+ (●) or 2·5 mM K_o^+ + NMG_o (□, TEA-sensitive current). Cell c5n15 (R_S = 2·2 MΩ).

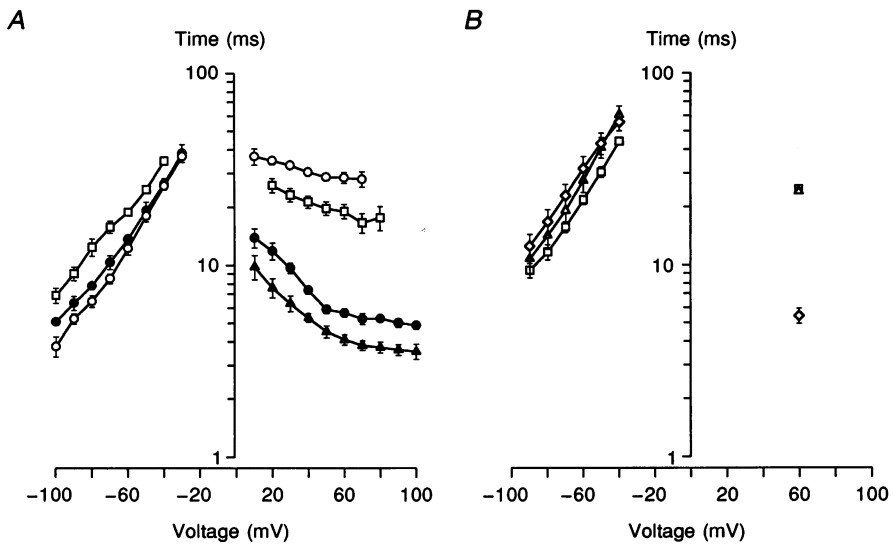

Figure 5. Kinetics in different ionic conditions, measured from TEA-sensitive currents

Activation kinetics are shown for voltages above 0 mV, and deactivation kinetics below 0 mV. *A*, kinetics with roughly symmetrical K^+ or Cs^+ solutions. *B*, kinetics with 100 mM Cs_i^+ and Cs_o^+ + K_o^+ mixtures. Currents were fitted to single exponentials (see Methods). ●, 25 mM K_i^+, 25 mM K_o^+; ○, 25 mM Cs_i^+, 25 mM Cs_o^+; △, 100 mM Cs_i^+, 1 mM K_o^+ + 119 mM Cs_o^+; ▲, 120 mM K_i^+, 120 mM K_o^+; □, 100 mM Cs_i^+, 120 mM Cs_o^+; ◇, 100 mM Cs_i^+, 25 mM K_o^+ + 95 mM Cs_o^+.

Effects of permeant ions on channel kinetics

Both activation and deactivation of the TEA-sensitive current were affected by permeant ions. In particular, activation was ~4-fold slower in Cs^+ than in K^+ (Fig. 5*A*). This was also apparent in the experiments with mixtures of K_o^+ and Cs_o^+, as activation was faster with 25 mM K_o^+ (+95 mM Cs_o^+) than with 120 mM Cs_o^+, while addition of only 1 mM K_o^+ did not speed activation detectably (Figs 3*A* and 5*B*). Activation was also affected by the concentration of permeant ion, being faster with higher concentrations of either K^+ or Cs^+ (Fig. 5*A*). With 25 mM K_i^+, activation at +60 mV was significantly faster in 25 mM K_o^+ ($\tau = 5{\cdot}1 \pm 0{\cdot}2$ ms, $n = 8$) than in 2·5 mM K_o^+ ($\tau = 8{\cdot}7 \pm 0{\cdot}2$ ms, $n = 8$). This observation, and the effect on kinetics with $K_o^+ + Cs_o^+$ mixtures, indicate that extracellular ions alone can affect activation.

Deactivation kinetics depended on the concentration of extracellular ion. Tail currents were faster in 25 mM Cs_o^+ than in 120 mM Cs_o^+ (Fig. 5*A*). Also for K_o^+, deactivation at −80 mV was faster in 2·5 mM K_o^+ ($\tau = 4{\cdot}2 \pm 0{\cdot}2$ ms) than in 25 mM K_o^+ ($\tau = 8{\cdot}0 \pm 0{\cdot}3$ ms, $n = 8$). In contrast to activation, deactivation kinetics did not vary between K_o^+ and Cs_o^+ (Fig. 5*A*), or among the $K_o^+ + Cs_o^+$ mixtures (Figs 3*A* and 5*B*). Deactivation was also similar with Cs_i^+ and K_i^+ (Fig. 5*A*). With 2·5 mM K_o^+, deactivation was not significantly different with 25 mM *versus* 120 mM K_i^+ (respectively, at −80 mV: $\tau = 4{\cdot}6 \pm 0{\cdot}7$ ms, $n = 4$; $\tau = 5{\cdot}9 \pm 0{\cdot}7$ ms, $n = 3$).

It might be expected that the changes in activation and deactivation rates would lead to shifts in the steady-state activation curve, but no clear effects were observed (Table 3).

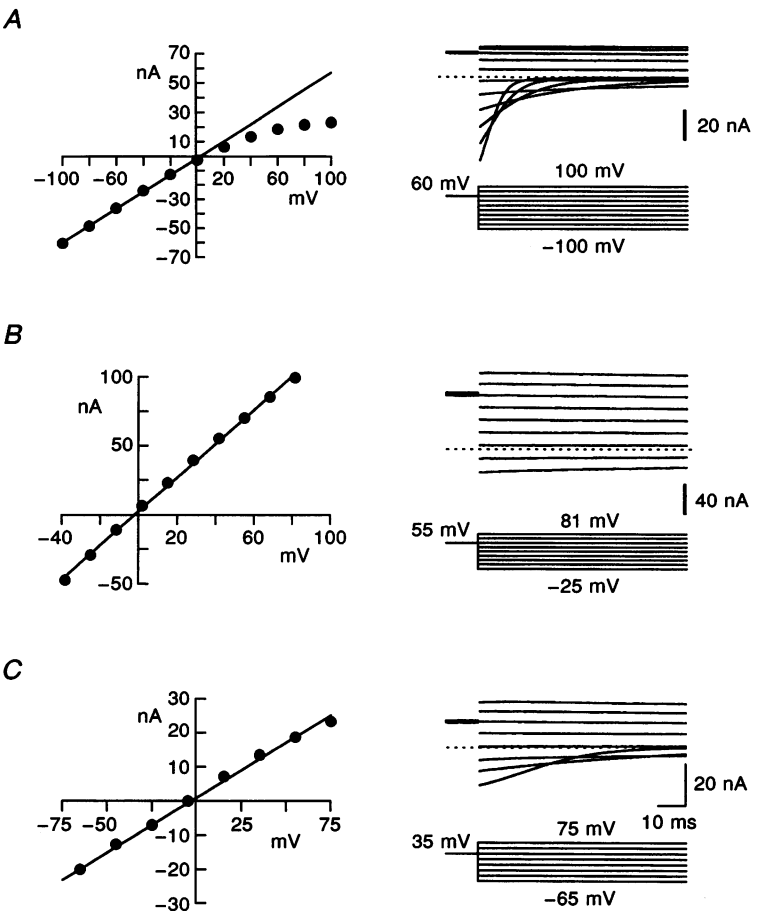

Figure 6. Block of K^+ current by intracellular NMG

A, in symmetrical 25 mM K^+ with NMG, the current was inwardly rectifying, as shown by a linear fit to the inward current (continuous line). Leak-subtracted currents from cell d6104 ($R_S = 1{\cdot}8$ MΩ). *B*, in symmetrical 120 mM K^+, the *I–V* relationship was linear. The continuous line is a linear fit to the *I–V* relationship from −20 to +80 mV, with voltage steps spaced every 13·3 mV. Currents from cell c5d26 ($R_S = 1$ MΩ). *C*, with 25 mM K^+ + intracellular sucrose, and 25 mM K_o^+ + NMG_o, the *I–V* relationship was nearly linear. The continuous line is a linear fit to the *I–V* relationship from −80 to +75 mV. Voltages were corrected for the +24·8 mV junction potential. The sigmoidal tail currents in *C* are indicative of poor voltage clamp due to the R_S voltage error ($R_S = 4{\cdot}5$ MΩ, voltage error ~1 mV nA^{-1}). Cell e5d19.

Table 4. Monovalent cation block of DR channels

	Intracellular X^+			Extracellular X^+		
Ion	K_{D0} (mM)	δ	n	Fraction blocked	n	Molecular weight
TEA	2·9 ± 0·2	0·33 ± 0·01 *‡§	4	—	—	130·3
NMG	469 ± 31	0·43 ± 0·01 ‡§	11	−0·04 ± 0·02	5	195·2
Arginine	487 ± 28	0·42 ± 0·02 ‡§	8	0·07 ± 0·06	5	174·2
Choline	157 ± 8	0·40 ± 0·01 ‡§	5	0·08 ± 0·04	5	104·2
$CH_3NH_3^+$	213 ± 8	0·53 ± 0·02 *‡	3	0·03 ± 0·02	4	31·1
Cs^+	156 ± 10	0·59 ± 0·03 *‡	5	0·87 ± 0·01	7	—
Li^+	134 ± 7	0·61 ± 0·01 *‡	3	0·02 ± 0·02	6	—
Na^+	328 ± 41	0·79 ± 0·01 *§	4	0·31 ± 0·01	6	—

For internal block, values significantly different from NMG (*), Na^+ (‡), or $CH_3NH_3^+$ (§) are noted. K_{D0} and δ were estimated using eqn (3). For Cs_i^+, Na_i^+ and Li_i^+, *I–V* relationships were fitted up to +80 mV, and to +100 mV for the other ions. Internal block was assessed with 25 mM K_i^+ + 100 mM X_i^+, except for TEA where 1 mM TEA was added to 25 mM K_i^+ + intracellular sucrose. The extracellular solution contained 25 mM K_o^+ + NMG_o. For symmetrical 25 mM K^+ plus impermeant or low permeability ions, the E_{rev} should have been 0 mV. It was assumed that the measured deviations in E_{rev} (−9 to 3 mV) were due to offsets and the fitted K_{D0} adjusted accordingly, i.e. K_{D0} corresponds to the K_D at E_{rev}. Block by extracellular cations was measured at −100 mV, for solutions applied by bath superfusion. Data for Na_o^+ and Cs_o^+ are from Block & Jones (1996*a*), with 88 mM K_i^+, and 25 mM K_o^+ (for Cs^+) or 10 mM K_o^+ (for Na^+). For other ions, extracellular block was tested with 120 mM K_i^+, and 25 mM K_o^+ + 92·5 mM X_o^+, with X^+ replacing NMG_o in 25 mM K_o^+ + NMG_o (Table 1). (See Table 2 for voltage-independent block by external TEA.)

Block by internal cations

With isotonic K_i^+, DR currents were large and difficult to voltage clamp adequately, so we wanted to replace some of the K^+ with an inert cation. We tried NMG, which does not permeate through DR channels from the outside (Block & Jones, 1996*a*), and is usually considered too large to enter an ion channel pore. Unexpectedly, in symmetrical 25 mM K^+ with NMG, the instantaneous *I–V* relationship was inwardly rectifying (Fig. 6*A*). As symmetrical K^+ was used, there could be no Goldman–Hodgkin–Katz rectification. We considered two other explanations, intrinsic rectification of the DR current, or block by an intracellular cation. One possible blocking ion was Mg^{2+}, which blocks a cloned delayed rectifier (Kv2.1; Lopatin & Nichols, 1994). However, free Mg_i^{2+} was only 0·22 mM in our usual intracellular solutions because of excess ATP (calculated with the FREECA program; Fabiato & Fabiato, 1979). Rectification was unchanged by removal of both Mg_i^{2+} and ATP (data not shown, $n = 3$). Also, no significant Mg_i^{2+} block was found with a total Mg_i^{2+} concentration of 20 mM, giving a free Mg_i^{2+} concentration of 10·7 mM (added to the 25 mM K_i^+ + intracellular sucrose solution), indicating a K_D value of > 1 M ($n = 4$, not shown).

With symmetrical 120 mM K^+, the *I–V* relationship was linear (Fig. 6*B*). In symmetrical 25 mM K^+ (with NMG_o, and intracellular sucrose to balance osmolality) there was a slight inward rectification, but far less than with NMG_i (Fig. 6*C*). The ratio of outward to inward currents (+75 *vs.* −75 mV) was 0·84 ± 0·02 ($n = 7$) with intracellular sucrose, compared with 0·57 ± 0·02 ($n = 10$) with NMG_i. Voltage error due to R_S was problematic in these experiments, as currents were very large with symmetrical 120 mM K^+, and the decrease in current with 25 mM K_i^+ + intracellular sucrose was paralleled by a 3- to 4-fold increase in R_S because of the low ionic strength pipette solution. However, these instantaneous *I–V* relationships do not have a negative slope region, so the effect of R_S error should be predictable. In particular, as R_S error is proportional to current amplitude, it will not make a rectifying *I–V* relationship appear linear. Because rectification was much stronger with NMG_i, it is concluded that NMG_i blocks the DR current.

We asked whether other cations could also block DR channels from the inside. A diverse set of monovalent cations (TEA, NMG, arginine, choline, $CH_3NH_3^+$, Li^+, Cs^+ and Na^+) all blocked DR channels in a voltage-dependent manner (Figs 7 and 8). Block was quantified using a version of the Woodhull (1973) model (eqn (3)), assuming that the *I–V* relationship was inherently linear and that any rectification stemmed from internal block. Except for TEA, block was low affinity, with K_{D0} ranging from 134 to 487 mM (Table 4). The apparent electrical distance (δ) was ~0·4 for NMG, arginine and choline, while the smallest organic cation tested ($CH_3NH_3^+$) seemed to penetrate slightly deeper into the membrane field. TEA was unique among the organic cations with the highest affinity and lowest $z\delta$ (Table 4). For most cations, internal block was too fast to resolve, being effectively instantaneous. $CH_3NH_3^+$, alone among the cations tested, had a small slow blocking component in addition to the 'instantaneous' block (Fig. 7*A*).

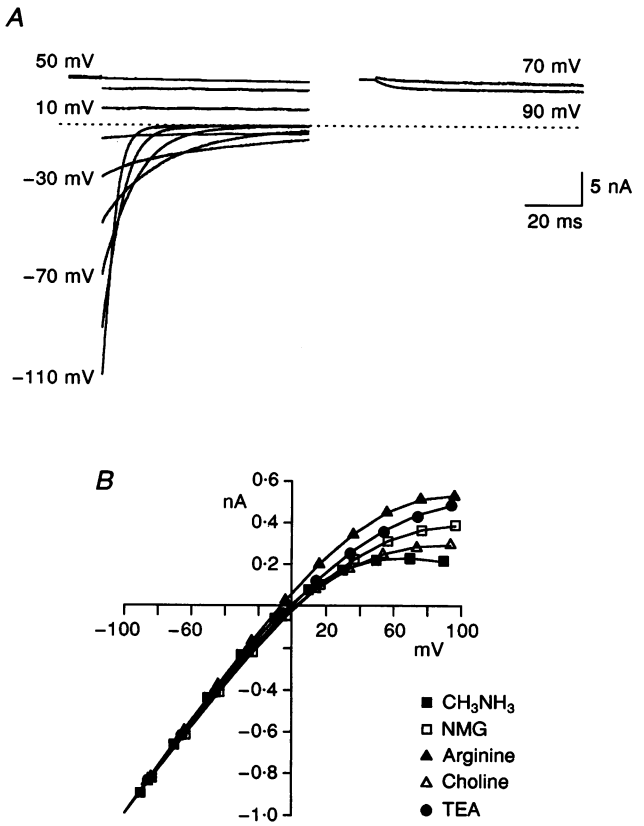

Figure 7. Block by large monovalent cations
A, currents with 25 mM K^+ + 100 mM $CH_3NH_3^+$ (both intracellular), and 25 mM K^+ + NMG (both extracellular), in 20 mV increments. Records on the right show the additional slow blocking component at +70 and +90 mV. Leak-subtracted currents evoked by a 90 ms step to +60 mV, from cell w6105 (R_S = 1·6 MΩ). *B*, normalized instantaneous *I–V* relationships with various intracellular cations at 100 mM, except for TEA (1 mM). *I–V* relationships were normalized to the current at −100 mV and are from leak-subtracted data. The curves are fits to the Woodhull model (eqn (3)).

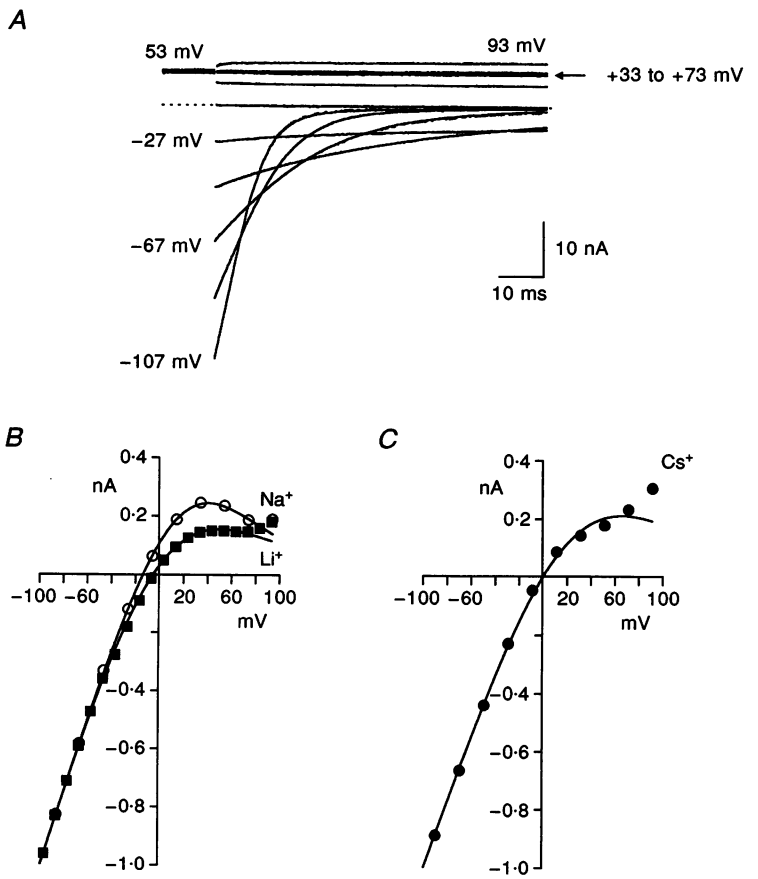

Figure 8. Block by small monovalent cations
A, current traces with 25 mM K_i^+ + 100 mM Li_i^+, and 25 mM K_o^+ + NMG_o, in 20 mV increments. Currents from +33 to +73 mV were of approximately equal amplitude (see arrow). Leak-subtracted currents evoked by a 90 ms step to +60 mV from cell c5d18 (R_S = 2·2 MΩ) with 1 mM extracellular saxitoxin.
B, normalized instantaneous *I–V* relationships with 100 mM Li_i^+ or Na_i^+ and 25 mM symmetrical K^+. *C*, normalized instantaneous *I–V* relationships with 25 mM K_i^+ + 100 mM Cs_i^+, and 25 mM K_o^+ + NMG_o. The curves are fits to eqn (3), including data up to +80 mV. Leak-subtracted data from cells c5d18 (Li_i^+), a6111 (Na_i^+) and e6112 (Cs_i^+).

The small inorganic cations also blocked the DR channels with low affinity, but at a larger $z\delta$ than the organic cations (Fig. 8 and Table 4).

We also examined currents with intracellular glucosamine. It was obtained as the hydrochloride, and as the pK_a for glucosamine is 7·8, it was titrated with ~0·2 mol KOH (mol glucosamine)$^{-1}$. To maintain K_i at 25 mM the total intracellular glucosamine concentration was 50 mM, of which 40 mM would be ionized. The rectification (+75 *vs.* −75 mV) was 0·81 ± 0·02 ($n = 4$), not significantly different from the 0·84 measured with intracellular sucrose. Because of the rectification with intracellular sucrose, the K_{D0} values for intracellular cations may be underestimated, but the $z\delta$ values should be affected little (the apparent $z\delta$ with intracellular sucrose was 0·4). The slight rectification with intracellular sucrose may reflect block by Tris (present at ~12 mM in all intracellular solutions; Table 1), or intrinsic rectification of the pore.

In order to test the symmetry of the pore, cations were tested for their ability to block DR channels from the extracellular solution. We have previously shown that both Na_o^+ and Cs_o^+ block DR channels in a voltage-dependent manner (Block & Jones, 1996*a*), and voltage-independent block by TEA_o is discussed above. The other organic cations did not block from the outside, as assessed in two ways. First, the rectification of the instantaneous *I–V* relationship was examined with 120 mM K_i^+ and 25 mM K_o^+ + 92·5 mM X_o^+, using the ratio (r) of the current measured 50 mV negative to reversal to the current 50 mV positive to the reversal potential. Despite the K^+ gradient (120 mM K_i^+ *vs.* 25 mM K_o^+), there was no rectification in 25 mM K_o^+ + extracellular sucrose ($r = 1·02 \pm 0·01$, $n = 15$), or with extracellular NMG, glucosamine, arginine, choline, $CH_3NH_3^+$ or Li^+ ($r = 0·95$–$0·99$, $n = 4$–6). External block was also tested by comparing, in the same cell, the inward currents at −100 mV in 25 mM K_o^+ + 92·5 mM X_o^+ to the current in 25 mM K_o^+ + extracellular sucrose (all with 120 mM K_i^+). Using that protocol, no block of DR channels was observed with extracellular NMG, arginine, choline, $CH_3NH_3^+$ or Li^+ (Table 4).

The data presented here on internal and external cation block were measured from leak-subtracted whole-cell K^+ currents (Figs 6–9). Difference currents ± TEA were inaccurate when R_S error was large, as the voltage error was ~5-fold smaller for the ~5-fold smaller currents in the presence of 10 mM TEA_o. Thus the total current and the current in TEA were actually recorded at different voltages. This produced artifacts in the difference currents, e.g. sigmoid tail currents. Despite this, Woodhull analysis of the TEA-sensitive current gave values similar to those for the leak-subtracted current. The one exception was Li_i^+, as the *I–V* relationship measured from TEA-sensitive currents did not have the small rising phase visible in Fig. 8*B* at strong depolarizations, and the $z\delta$ was higher (0·77 ± 0·02, $n = 3$).

Voltage-dependent block is often assumed to imply that block occurs within the ion conduction pathway, the only ion-accessible portion of the channel known to be in the membrane field. The 'knock-off' effect, where block by an internal cation is decreased by increasing K_o^+, provides additional evidence that the site of block is in the pore (Armstrong, 1971; Lopatin & Nichols, 1994). To test for this, NMG_i block was assessed in 120 mM K_o^+ *vs.* 25 mM K_o^+ in the same cell (Fig. 9). Despite the decreased driving force, outward currents beyond +60 mV were larger in 120 mM K_o^+ ($n = 4$), implying weaker block in high K_o^+. In contrast, little or no effect of K_o^+ was observed on outward currents at strongly depolarized voltages in the absence of NMG_i: at +99 mV, with intracellular sucrose, currents were 9 ± 12% larger with 120 mM K_o^+ than with 25 mM K_o^+ ($n = 3$), compared with 60 ± 21% larger with NMG_i ($n = 6$).

DISCUSSION

Isolation of DR current

With Cs^+ as the charge carrier, there appear to be two kinetically and pharmacologically distinct currents under our recording conditions. Approximately 85% of the current deactivates rapidly and is highly sensitive to TEA, and the remaining slower tail current is at least 10-fold less sensitive to TEA. We term the predominant current a delayed rectifier (DR) current, as it resembles the DR currents seen with K^+ in these (Adams *et al.* 1982) and other cells. Although we cannot be certain from macroscopic current data that the TEA-sensitive DR current reflects the activity of a single type of K^+ channel, the DR tail currents

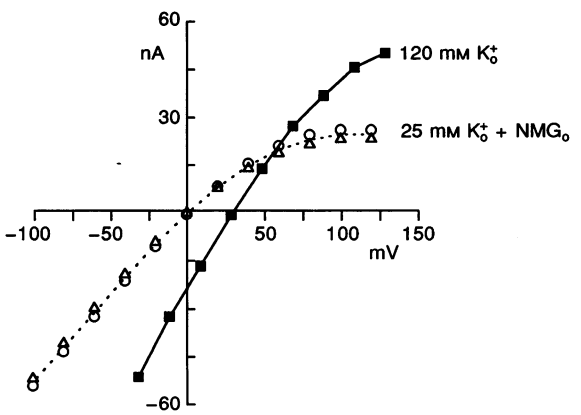

Figure 9. Knock-off of intracellular NMG block by K_o^+
Instantaneous tail currents were recorded with 25 mM K_i^+ + 100 mM NMG_i. Outward currents were greater in 120 mM K_o^+ than in 25 mM K_o^+ + NMG_o (control and recovery). The dotted line is the average current in 25 mM K_o^+ + NMG_o. The continuous line connects the data points in 120 mM K_o^+. Leak-subtracted data from cell e6311 ($R_S = 1·2$ MΩ).

can be well described by a single exponential over a considerable voltage range, either with K^+ (Greene & Jones, 1993) or with Cs^+, so if multiple channels are present, they cannot be easily distinguished kinetically. With Cs^+, where ~15% of the total current was TEA-resistant, the difference current ± 10 mM TEA was considered to be the best measure of DR current, but the main results reported here were observed either for the total leak-subtracted current or for the TEA difference current. For example, slow activation kinetics in Cs^+ were also observed with leak-subtracted currents: at +60 mV, with 100 mM Cs^+_i and 120 mM Cs^+_o, $\tau = 12{\cdot}1 \pm 0{\cdot}6$ ms, $n = 4$; *vs.* $\tau = 4{\cdot}8 \pm 0{\cdot}2$ ms, $n = 4$, with 120 mM K^+_o and K^+_i. Only 5% of the current is TEA resistant with K^+ (Greene & Jones, 1993), so as in the previous study of DR currents with K^+_i (Block & Jones, 1996*a*), it was not necessary to use difference currents for the experiments reported here on block of K^+ currents by intracellular cations.

Isolation of DR channels is more difficult to evaluate with Na^+ as the charge carrier, as the currents were not sensitive to TEA. However, the currents with Na^+ closely resemble those from the heterologously expressed Kv2.1 channel, where current isolation is not an issue (Ikeda & Korn, 1995): TEA sensitivity was lost with Na^+_o (and no K^+_o or K^+_i), but physiological concentrations of K^+_o restored TEA sensitivity, and the current deactivated more slowly with Na^+_o (and no K^+_o or K^+_i). Based on this similarity, we presume that the TEA-resistant currents in these experiments with Na^+ result primarily from DR channels that have lost TEA sensitivity, rather than a distinct, fundamentally TEA-resistant current. However, it is possible that part of the current recorded with Na^+ is not through DR channels, but perhaps through the channel(s) that are TEA resistant with Cs^+ as charge carrier. For this reason, currents with Na^+ were not examined in detail in this study.

Permeation of Na^+ and Cs^+

Rat superior cervical ganglion, chick dorsal root ganglion, and Kv2.1 K^+ channels all have high conductances to Na^+ when K^+ is removed (Zhu & Ikeda, 1993; Callahan & Korn, 1994; Korn & Ikeda, 1995). This is not a universal property of all K^+ channels, as Kv1.5 channels do not conduct significant Na^+ even in the absence of K^+ (Korn & Ikeda, 1995). Korn & Ikeda (1995) argued that K^+ selectivity was mediated by competition in a multi-ion pore and that, at least in Kv2.1, there was no inherent rejection of Na^+ by the channel. The bullfrog DR channel seems to employ a similar competitive mechanism for ion selectivity. This is reminiscent of Ca^{2+} channels, in which Ca^{2+} selectivity is achieved by a high affinity for Ca^{2+} compared with Na^+, and high ion flux rates are a consequence of ion–ion interaction in a multi-ion pore (Almers & McCleskey, 1984; Hess & Tsien, 1984). Although the two-site model for Ca^{2+} channel permeation has recently come into question (Armstrong & Neyton, 1992; Yang, Ellinor, Sather, Zhang & Tsien, 1993), the idea of competition between permeant ions has not.

However, the DR channel does not become a completely non-selective cation channel in the absence of K^+. Comparing isotonic Cs^+ or Na^+ with K^+ (in separate cells), G_{Cs}/G_K was $0{\cdot}13 \pm 0{\cdot}03$, and G_{Na}/G_K was $0{\cdot}07 \pm 0{\cdot}02$, noting that G_K is underestimated because of R_S error. G_{Cs}/G_K is comparable to P_{Cs}/P_K, and to G_{Cs}/G_K with K^+_i (Block & Jones, 1996*a*). Therefore, the selectivity of the DR channel for K^+ over Cs^+ does not require Cs^+–K^+ interaction, although the dramatic anomalous mole fraction effect (Fig. 4) demonstrates that Cs^+–K^+ competition can be strong. For Na^+, G_{Na}/G_K is clearly larger than P_{Na}/P_K ($0{\cdot}022 \pm 0{\cdot}005$ with Na^+_i; $0{\cdot}0093 \pm 0{\cdot}0002$ with K^+_i; Block & Jones, 1996*a*), suggesting a greater role for competition in selectivity for K^+ over Na^+.

In our previous study of DR currents using K^+_i, we observed several multi-ion pore behaviours, but only a small anomalous mole fraction effect in $K^+_o + Rb^+_o$ mixtures (Block & Jones, 1996*a*). The large anomalous mole fraction effect observed here for $K^+_o + Cs^+_o$ confirms our conclusion that the DR channel is a multi-ion pore.

For studies of Na^+ and Ca^{2+} currents, intracellular K^+ is often replaced by Cs^+. The permeability of K^+ channels to Cs^+ explains why the block of K^+ channels is often incomplete (e.g. Jones, 1987). Actually, a mixture of Cs^+_i and K^+_i might prevent current through K^+ channels more effectively than Cs^+_i alone. In addition, our results rationalize the use of Cs^+_i and TEA_o in combination, although even this does not completely block K^+ channel currents (Figs 1 and 2).

Effects of permeant ions on channel gating and block

Permeant ions affected both activation and deactivation rates of DR channels. The most dramatic effect was ~4-fold slower activation with Cs^+_o *vs.* K^+_o. Increases in $[K^+]_o$ or $[Cs^+]_o$ also speeded activation by ~2-fold. Deactivation was slower at high extracellular permeant ion concentration, with no clear difference between K^+ and Cs^+. However, deactivation of DR channels can depend on ion species, as it was slowed 1·4-fold by equimolar replacement of K^+_o with Rb^+_o (data from Block & Jones, 1996*a*), and deactivation was also slow with Na^+_o and Na^+_i (Fig. 4*A*). The changes in kinetics cannot be attributed to R_S errors.

In many systems, permeant ions affect K^+ channel deactivation, but effects on activation have been reported only rarely. Replacement of K^+_o with Rb^+_o can slow K^+ channel deactivation (Swenson & Armstrong, 1981), by up to 14-fold (Shapiro & DeCoursey, 1991), with no effect on activation. Similarly, Cs^+ slowed deactivation relative to K^+ (1·5-fold) in the squid axon, but did not affect activation kinetics (Matteson & Swenson, 1986). However, for Ca^{2+}-activated K^+ channels of skeletal muscle, internal or external Cs^+ speeded opening and (in contrast to the results with DR channels) slowed closing (Neyton & Pelleschi, 1991; Demo & Yellen, 1992). It is likely that these phenomena reflect effects of ion occupancy on the conformational changes involved in channel gating, but the detailed mechanisms remain to be established.

In addition to affecting gating kinetics, the ionic environment of the channel also affected block by TEA_o. Occupancy of the pore by K^+ appears to favour a conformation that binds TEA_o strongly (see also Ikeda & Korn, 1995). One possibility is that the channel pore is relatively rigid, with distinct, slowly interconverting TEA_o-sensitive and TEA_o-resistant states. However, TEA_o block and gating did not always change in parallel, as replacement of K^+ with Cs^+ affected activation kinetics but not TEA_o block (Fig. 5; Table 2). This suggests that ion occupancy can induce several several different open conformations, perhaps reflecting a flexible pore with several rapidly interconverting states, as proposed by Yang *et al.* (1993) for Ca^{2+} channels. However, for K^+ channels, the effects of permeant ions on gating and TEA_o block imply that the effects of the conformational change must extend beyond the 'deep' pore (Ikeda & Korn, 1995).

Asymmetric nature of the pore

The DR channel pore was blocked by every monovalent cation tested from the intracellular solution (except K^+, and possibly glucosamine) while only TEA, Na^+, and Cs^+ blocked DR channels from the outside. These data indicate that the pore is asymmetric, and the inner mouth of the pore is non-selective. Block by TEA_i has also suggested a wide inner pore (Armstrong, 1971; French & Shoukimas, 1981; Taglialatela, Vandongen, Drewe, Joho, Brown & Kirsch, 1991), but that interpretation is complicated by possible interactions of the aliphatic groups of TEA (and its long-chain derivatives) with hydrophobic regions of the channel protein. In fact, the hydrophobicity of an amino acid residue in the S6 transmembrane region strongly affects binding of TEA_i and derivatives (Choi, Mossman, Aubé & Yellen, 1993). The hydrophilic cations used here are more likely to be restricted to the water-filled pore, and thus provide stronger evidence that the inner mouth of the pore is wide. The inner mouth of the pore now has two constraints: it must be large enough to hold a large cation such as NMG, yet narrow enough that the membrane voltage can be 'felt' by the blocking ion. Since the voltage drop is steeper in the narrower regions of a pore, it is particularly striking that a cation as large as NMG can penetrate so deeply (43% of the electrical distance).

There have been many previous reports of voltage-dependent block of K^+ channels by small inorganic cations from the intracellular solution, including Na_i^+ and Cs_i^+ (Bezanilla & Armstrong, 1972; French & Wells, 1977; Yellen, 1984; Cukierman, Yellen & Miller, 1985; French & Shoukimas, 1985; Cecchi, Wolff, Alvarez & Latorre, 1987; Lopatin & Nichols, 1994). Many K^+ channels are also blocked by TEA_i (Armstrong, 1971; Hille, 1992). However, block by a wide variety of internally applied organic cations has been shown previously only for the K^+ channel of the squid giant axon (French & Shoukimas, 1981, 1985).

The voltage dependence of block varied considerably among the various intracellular blocking ions (Table 4). There is a rough inverse correlation between $z\delta$ and ion size, which might suggest that these ions do not bind to a specific site in the pore (except possibly for TEA), but instead are 'wedged' into the pore by the electrical driving force. However, there are two potential problems with this literal interpretation. First, the simplified Woodhull (1973) model is not strictly valid for Na^+ and Cs^+ block, as it assumes that the blocking ion is completely impermeant (eqn (3)). The rising phase in the instantaneous I–V relationships in Fig. 8, which is clearest for Cs^+ (Fig. 8*C*), probably reflects the 'blocking' ion being forced through the pore by strong depolarization, as reported for Na^+ in the squid axon K^+ channel (French & Wells, 1977). Also, if two (or more) blocking ions were in the pore at once, $z\delta$ would be overestimated. That possibility is most realistic for the small inorganic cations (Na^+, Cs^+ and Li^+), which could explain why their $z\delta$ values are higher than for the larger inorganic cations.

Because internal solutions were not exchanged in the same cell, voltage-independent block by internal cations could not be assessed. Voltage-independent block would have reduced the current amplitude by a fixed percentage at all voltages. Experimentally, this set of cells would have a lower whole-cell conductance, which might not have been obviously different from control.

These results, in conjunction with previous data on DR channel permeation (Block & Jones, 1996*a*), suggest a physical picture of the channel. There is robust and varied evidence of multi-ion pore behaviour for DR channels. The pore is asymmetric, with an outer pore narrow enough to exclude all organic cations tested. In contrast, the inner pore is wide enough to accommodate all the cations tested, and yet narrow enough to sense the transmembrane voltage. The channel selects by competition, and does not intrinsically reject ions such as Na^+. Because TEA_o block depends on the permeating ion, the pore seems to adopt different conformations for different permeating ions. The effects of permeant ions on channel kinetics suggest that the conformational changes in the pore affect other regions of the channel.

Adams, P. R., Brown, D. A. & Constanti, A. (1982). M-currents and other potassium currents in bullfrog sympathetic neurones. *Journal of Physiology* **330**, 537–572.

Almers, W. & McCleskey, E. W. (1984). Non-selective conductance in calcium channels of frog muscle: calcium selectivity in a single-file pore. *Journal of Physiology* **353**, 585–608.

Armstrong, C. M. (1971). Interaction of tetraethylammonium ion derivatives with the potassium channels of giant axons. *Journal of General Physiology* **58**, 413–437.

Armstrong, C. M. & Neyton, J. (1992). Ion permeation through calcium channels, a one-site model. *Annals of the New York Academy of Sciences* **635**, 18–25.

Barry, P. H. & Lynch, J. W. (1991). Liquid junction potentials and small cell effects in patch-clamp analysis. *Journal of Membrane Biology* **121**, 101–117.

Bezanilla, F. & Armstrong, C. M. (1972). Negative conductance caused by entry of sodium and cesium ions into the potassium channels of squid axons. *Journal of General Physiology* **60**, 588–608.

Block, B. M. & Jones, S. W. (1996*a*). Ion permeation and block of M-type and delayed rectifier potassium channels: Whole-cell recordings from bullfrog sympathetic neurons. *Journal of General Physiology* **107**, 473–488.

Block, B. M. & Jones, S. W. (1996*b*). Delayed rectifier currents in bullfrog sympathetic neurons with intracellular Cs^+. *Biophysical Journal* **70**, A188.

Callahan, M. J. & Korn, S. J. (1994). Permeation of Na^+ through a delayed rectifier K^+ channel in chick dorsal root ganglion neurons. *Journal of General Physiology* **104**, 747–771.

Cecchi, X., Wolff, D., Alvarez, O. & Latorre, R. (1987). Mechanism of Cs^+ blockade in a Ca^{2+}-activated K^+ channel from smooth muscle. *Biophysical Journal* **52**, 707–716.

Choi, K. L., Mossman, C., Aubé, J. & Yellen, G. (1993). The internal quaternary ammonium receptor site of *Shaker* potassium channels. *Neuron* **10**, 533–541.

Cukierman, S., Yellen, G. & Miller, C. (1985). The K^+ channel of sarcoplasmic reticulum: a new look at Cs^+ block. *Biophysical Journal* **48**, 477–484.

Demo, S. D. & Yellen, G. (1992). Ion effects on gating of the Ca^{2+}-activated K^+ channel correlate with occupancy of the pore. *Biophysical Journal* **61**, 639–648.

Fabiato, A. & Fabiato, F. (1979). Calculator programs for computing the composition of the solutions containing multiple metals and ligands used for experiments in skinned muscle cells. *Journal de Physiologie* **75**, 463–505.

French, R. J. & Shoukimas, J. J. (1981). Blockage of squid axon potassium conductance by internal tetra-*N*-alkylammonium ions of various sizes. *Biophysical Journal* **34**, 271–291.

French, R. J. & Shoukimas, J. J. (1985). An ion's view of the potassium channel. The structure of the permeation pathway as sensed by a variety of blocking ions. *Journal of General Physiology* **85**, 669–698.

French, R. J. & Wells, J. B. (1977). Sodium ions as blocking agents and charge carriers in the potassium channel of the squid giant axon. *Journal of General Physiology* **70**, 707–724.

Greene, K. J. & Jones, S. W. (1993). An allosteric model for the delayed rectifier potassium current of frog sympathetic neurons. *Biophysical Journal* **64**, A312.

Hess, P. & Tsien, R. W. (1984). Mechanism of ion permeation through calcium channels. *Nature* **309**, 453–456.

Hille, B. (1992). *Ionic Channels of Excitable Membranes*, 2nd edn, p. 607. Sinauer Associates Inc., Sunderland, MA, USA.

Ikeda, S. R. & Korn, S. J. (1995). Influence of permeating ions on potassium channel block by external tetraethylammonium. *Journal of Physiology* **486**, 267–272.

Jones, S. W. (1987). Sodium currents in dissociated bullfrog sympathetic neurones. *Journal of Physiology* **389**, 605–627.

Jones, S. W. (1991). Time course of receptor–channel coupling in frog sympathetic neurons. *Biophysical Journal* **60**, 502–507.

Jukes, T. H. (1964). *Choline*. In *Kirk-Othmer Encyclopedia of Chemical Technology*, 2nd edn, ed. Grayson, M., pp. 403–413. John Wiley & Sons Inc., New York.

Juvet, R. S. Jr (1959). The *N*-methylglucamine complexes. I. The lead *N*-methylglucamine system. *Journal of the American Chemical Society* **81**, 1796–1801.

Korn, S. J. & Ikeda, S. R. (1995). Permeation selectivity by competition in a delayed rectifier potassium channel. *Science* **269**, 410–412.

Kuffler, S. W. & Sejnowski, T. J. (1983). Peptidergic and muscarinic excitation at amphibian sympathetic synapses. *Journal of Physiology* **341**, 257–278.

Lopatin, A. N. & Nichols, C. G. (1994). Internal Na^+ and Mg^{2+} blockade of DRK1 (Kv2.1) potassium channels expressed in *Xenopus* oocytes: inward rectification of a delayed rectifier. *Journal of General Physiology* **103**, 203–216.

Martell, A. E. & Smith, R. M. (1975). *Critical Stability Constants*, vol. 2, Amines, p. 415. Plenum Press, New York.

Matteson, D. R. & Swenson, R. P. Jr (1986). External monovalent cations that impede the closing of K channels. *Journal of General Physiology* **87**, 795–816.

Neher, E. (1992). Correction for liquid junction potentials in patch clamp experiments. *Methods in Enzymology* **207**, 123–31.

Neyton, J. & Pelleschi, M. (1991). Multi-ion occupancy alters gating in high-conductance, Ca^{2+}-activated K^+ channels. *Journal of General Physiology* **97**, 641–665.

Shapiro, M. S. & DeCoursey, T. E. (1991). Permeant ion effects on the gating kinetics of the type L potassium channel in mouse lymphocytes. *Journal of General Physiology* **97**, 1251–1278.

Stampe, P. & Begenisich, T. (1996). Unidirectional K^+ fluxes through recombinant *Shaker* potassium channels expressed in single *Xenopus* oocytes. *Journal of General Physiology* **107**, 449–457.

Swenson, R. P. Jr & Armstrong, C. M. (1981). K^+ channels close more slowly in the presence of external K^+ and Rb^+. *Nature* **291**, 427–429.

Taglialatela, M., Vandongen, A. M. J., Drewe, J. A., Joho, R. H., Brown, A. M. & Kirsch, G. E. (1991). Patterns of internal and external tetraethylammonium block in four homologous K^+ channels. *Molecular Pharmacology* **40**, 299–307.

Woodhull, A. M. (1973). Ionic blockage of sodium channels in nerve. *Journal of General Physiology* **61**, 687–708.

Yang, J., Ellinor, P. T., Sather, W. A., Zhang, J.-F. & Tsien, R. W. (1993). Molecular determinants of Ca^{2+} selectivity and ion permeation in L-type Ca^{2+} channels. *Nature* **366**, 158–161.

Yellen, G. (1984). Ionic permeation and blockade in Ca^{2+}-activated K^+ channels of bovine chromaffin cells. *Journal of General Physiology* **84**, 157–186.

Zhu, Y. & Ikeda, S. R. (1993). Anomalous permeation of Na^+ through a putative K^+ channel in rat superior cervical ganglion neurones. *Journal of Physiology* **468**, 441–461.

Acknowledgements

Thiw work was supported in part by NIH grant NS 24471 to S.W.J., who was an Established Investigator of the American Heart Association. B.M.B. was also supported by a fellowship from an NIH Medical Scientist Training Program.

Author's email address

S. W. Jones: swj@po.cwru.edu

Received 12 September 1996; accepted 19 November 1996.